Imaging of tophi with an extremity-dedicated MRI system

F. Paparo[1], G. Zampogna[2], E. Fabbro[1], M. Parodi[2], R. Andracco[2], G. Ferrero[1], G. Garlaschi[1], M.A. Cimmino[2]

[1]Sezione di Diagnostica per Immagini and [2]Clinica Reumatologica, Dipartimento di Medicina Interna (DIMI), Università di Genova, Genoa, Italy.

Abstract

Objectives

To describe the MRI features of gout tophi in the soft-tissues or joints of the limbs by low-field extremity-dedicated MRI.

Methods

Nine consecutive patients, 8M/1W, affected by chronic tophaceous gout were studied. Mean patients' age was 71.3±11.5 years, mean disease duration 98.1±44.9 months, and mean serum uric acid concentration 9.2±2.8 mg/L. Diagnosis was based on the ACR classification criteria for gout, and by identification of MSU crystals in the tophi and synovial fluid. Conventional radiograms and MRI with an extremity-dedicated system were obtained of the joint areas involved by tophi.

Results

At T1 weighted MRI images, all tophi showed a homogeneous intermediate signal intensity, similar to that of muscle. Conversely, in T2 weighted images, a wide spectrum of signal intensity patterns was observed. The pattern of contrast enhancement was variable from intense homogeneous to peripheral and heterogeneous. Capsulo-ligamentous structures were often thickened and degenerated and, on occasion, could be recognised as inhomogeneous, hypointense ribbon-shaped elements in the context of the tophus. In only two cases, tendons were infiltrated by tophaceous matter. Bone marrow oedema (BME) and erosions were seen in 8 out of 10 bones adjacent to tophi.

Conclusions

The MRI appearance of gout tophi using an extremity-dedicated machine is similar to that described in the literature using whole body machines. BME adjacent to the tophus was a frequent finding. This technique may occasionally help in the differential diagnosis of nodules and in the follow-up of the disease. It also represents a useful tool to investigate the pathogenesis of gout and to better understand its clinical progression.

Key words

gout, tophi, MRI, extremity-dedicated MRI

Francesco Paparo, MD
Giuseppe Zampogna, MD
Emanuele Fabbro, MD
Massimiliano Parodi, MD
Romina Andracco, MD
Giulio Ferrero, MD
Giacomo Garlaschi, MD
Marco A. Cimmino, MD

Please address correspondence and reprint requests to:
Prof. Marco A. Cimmino,
Clinica Reumatologica,
Dipartimento di Medicina Interna,
Università di Genova,
Viale Benedetto XV no.6,
16132 Genova, Italy.
E-mail: cimmino@unige.it

Received on September 2, 2010; accepted in revised form on February 11, 2011.

Competing interests: none declared.

Introduction

Gout, a common form of microcrystalline arthropathy, is a metabolic disease that may result in the deposition of uric acid salts and crystals in and around the joints and soft tissues. The disease course can be summarised in four clinical phases, asymptomatic hyperuricemia, acute gouty arthritis, intercritical gout and chronic tophaceous gout (1). Tophi are extracellular deposits of monosodium urate crystals (MSU) surrounded by foreign-body giant cells and mononuclear cells, which form a granuloma-like structure (2). In chronic tophaceous gout, they can occur in the articular cartilage, subchondral bone, synovial membrane, and capsula; as well as in periarticular tissues, such as tendons, ligaments, and bursae, particularly in the olecranon and prepatellar regions (3).

Tophi apparently take years to develop during the course of gout. On occasion, they may be seen in the absence of arthritis, as the initial manifestation of gout, a condition defined as "gout nodulosis" (1, 4).

The diagnosis of gout is usually based on clinical presentation and laboratory findings, with the gold standard represented by demonstration of MSU crystals in the joint fluid or tophi by polarising light microscopy (2, 3, 5). Imaging has a complementary role, usually limited to late disease. Radiography is the primary imaging tool. In the late stage of the disease, it shows punched-out, juxta-articular, lytic lesions that are associated with only minimal reactive new bone formation in the absence of juxta-articular osteoporosis (1, 6). Ultrasonography (US) is rarely used in clinical practice in patients with gout. At US examination, tophi appear as heterogeneous masses containing hypoechoic areas surrounded by hyperechoic tissue (7, 8). Occasional hyperechoic calcific deposits may be seen. US is helpful to detect small joint effusion and to guide joint aspiration (4). CT has not been extensively used in the study of chronic tophaceous gout. Gerster *et al*. demonstrated that tophi have a specific attenuation value ranging from 160 to 200 Hounsfield Units or above (8). CT is considered to be more sensitive than plain radiography in the detection and evaluation of cortical bone erosions associated with tophi, an assumption that has been recently challenged (9).

MRI is used as the primary imaging modality only in the rare cases of gout involving the spine (2), where a solitary tophus, presenting as a soft tissue mass, may be confused with a tumour (10). Few papers have evaluated the MRI appearance of peripheral tophi using high field total body machines (8, 10-14). The purpose of our work is to describe the MRI features of gout tophi of soft-tissues or joints of the limbs by low-field extremity-dedicated MRI.

Patients and methods

Nine consecutive patients affected by chronic tophaceous gout were studied. They included eight men and one woman with mean age 71.3±11.5 years, mean disease duration 98.1±44.9 months, and mean serum uric acid 9.2±2.8 mg/L. Physical examination was performed at baseline visit in all patients. Gout was diagnosed according to the ACR classification criteria (15) and by identification of MSU crystals in the tophi and synovial fluid. All patients had long-lasting disease, except for the lady in whom a DIP tophus appeared only 2 months before her first visit, as the initial manifestation of gout. Serum uric acid was elevated at the time of the first visit in 7/9 patients.

Conventional radiograms of the joints involved by tophi were obtained. MRI was performed with a 0.2T extremity-dedicated system (Artoscan C, Esaote, Genova, Italy) equipped with a permanent magnet and dedicated coils. In all examinations turbo-three-dimensional T1-weighted (TR/TE 35/16, FOV 140x140x100), spin-echo T1-weighted, short tau inversion recovery (TR/TE 1500/24, TI 85, FOV 200x180), turbo spin-echo (TE=80, TR=2800, FOV 160x160) and gradient-echo T2-weighted (TR/TE 950/22, Flip Angle 40°) sequences were used in orthogonal spatial planes. Turbo3D T1-weighted sequences were obtained before and after intravenous infusion of a paramagnetic contrast agent (Magnevist®, Bayer Schering Pharma AG, Germany). Contrast agent was avoided in patients with renal insufficiency. The study had the approval of

Table I. Characteristics of the tophi examined in the patients of the present study. Measures are taken in mm and include the cranio-caudal, latero-lateral, and antero-posterior distances (MCP: metacarpophalangeal joint; DIP: distal interphalangeal joint; MTP: metatarsophalangeal joint; BME: bone marrow edema; CE: contrast enhancement).

Location	Size (mm)	MRI pattern T1-weighted sequences	MRI pattern T2-weighted sequences	MRI pattern after contrast agent infusion	Extraarticular tissues	BME	Erosion
Second MCP	40x14x38	homogeneous intermediate signal intensity, similar to muscle	intermediate to low heterogeneous signal intensity	heterogeneous CE with an intermediate to low signal intensity. Thin, peripheral linear area of marked CE	thickening and degeneration of the capsulo-ligamentous structures. Dislocation of the second finger extensor tendon	+	+
Second MCP	35x40x30	homogeneous intermediate signal intensity, similar to muscle	intermediate to low heterogeneous signal intensity	ND	complete disruption of capsulo-ligamentous structures. Ventral dislocation of the proximal phalanx	+	+
Second MCP	25x30x20	homogeneous intermediate signal intensity, similar to muscle	intermediate to low heterogeneous signal intensity	ND	disruption of the radial, and thickening and degeneration of the ulnar capsulo-ligamentous structures.	+	+
Second DIP	13x16x17	homogeneous intermediate signal intensity	intermediate homogeneous signal intensity	ND	collateral ligaments and capsule are not clearly appreciable	+	+
Third DIP	17x16x16	homogeneous intermediate signal intensity	intermediate homogeneous signal intensity	ND	collateral ligaments and capsule are not clearly appreciable	+	+
Extensor carpi ulnaris tendon	25x10x9	homogeneous intermediate signal intensity	heterogeneous intermediate to low signal intensity	heterogeneous CE of the tophus but not of the tendon	enlargement of tendon axial diameter with dislocation of retinacular structures. Tenosynovitis	+	+
Elbow	66x36x17	homogeneous intermediate signal intensity, similar to muscle	high signal intensity area on the radial portion	heterogeneous enhancement with an intermediate to low signal intensity	compression of the anconeus and extensor carpi ulnaris muscular bellies. Olecranic bursitis	–	+
Patellar tendon	10x5x5	not visible	high signal intensity	ND	normal	–	–
First MTP	24x8x10	homogeneous intermediate signal intensity, similar to muscle, with small areas of absent signal	intermediate to low heterogeneous signal intensity pattern, with small areas of absent signal	ND	thickening of the medial collateral capsular ligament, with non homogeneous signal intensity and preservation of its continuity	+	–
First MTP	36x36x30	homogeneous intermediate signal intensity, similar to muscle	intermediate to low heterogeneous signal intensity pattern	ND	circumferential asymmetric involvement of the first MTF joint with thickening and degeneration of medial and lateral capsulo-ligamentous structures	+	+

the ethical committee of the University of Genova and the patients gave their informed consent for the MRI procedure.

Results

An abridged table of location, dimension, and MRI findings of tophi and surrounding tissues seen in our group of patients is reported (Table I). Ten tophi from 9 patients were studied; all of them were evaluable at clinical examination except for the one located in the patellar tendon. At T1 weighted MRI images, all tophi showed a homogeneous intermediate signal intensity, similar to that of muscle. Conversely, at T2 weighted images, a wide spectrum of signal intensity patterns, which probably reflected their variable composition and relative proportions of MSU crystals, proteins, fibrous tissue, and haemosiderin was observed.

Juxta-articular tophi with involvement of the second metacarpophalangeal joint (MCP) and extension into surrounding soft tissues were seen in 3 patients. In one of them, a large single tophus was present; the remaining two patients had multiple tophi in different parts of the body. MRI demonstrated

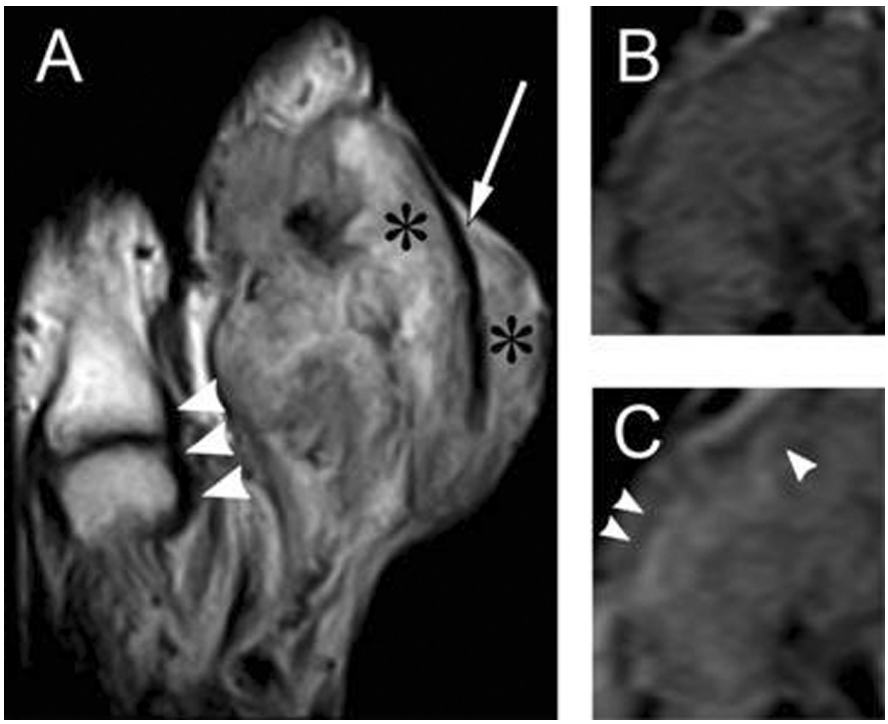

Fig. 1. A. The large inhomogeneous tophus of the second MCP joint (asterisk) induces diastasis and dislocation of the second finger extensor tendon (arrow), which is visible on the dorsal aspect of the mass with preservation of its continuity. Note the preservation of the capsule-legamentous components of the first MCP joint (arrowheads), whereas these structures disappeared in the second MCP (TSE T2-weighted sagittal sequence). SE T1-weighted coronal sequences before (**B**) and after (**C**) i.v. administration of contrast agent demonstrate the heterogeneous linear enhancement (small arrowheads), suggestive of a vascularised region of the tophus periphery.

Fig. 2. A) radiograph of the distal interphalangeal joint of the left hand showing "cloudlike" soft tissue swelling (arrowheads, see also **B** and **C**) and a para-articular erosion with overhanging edges (arrow), sclerotic margins, asimmetric relative preservation of the joint space, and lack of osteoporosis. **B**) Gradient-recalled Echo T2-weighted coronal sequence and **C**) Short Tau Inversion Recovery (STIR) coronal sequence showing a heterogeneous high signal intensity pattern throughout the lesion. Bone marrow edema is appreciable in the diaphysis of the middle and distal phalanges. **D**) STIR axial sequence; tophaceous tissue is visible on both articular sides, with an almost circumferential involvement, but with asymmetric distribution.

a homogeneous intermediate signal intensity pattern, similar to that of muscle, on T1-weighted sequences. On T2-weighted images, these lesions showed an intermediate to low heterogeneous signal intensity pattern (Fig. 1 A). On Turbo-3D, T1-weighted sequences after intravenous administration of the contrast agent, a heterogeneous peripheral enhancement pattern was seen, with a thin, peripheral linear area of marked contrast enhancement, suggestive of a highly vascularised area (Fig. 1 B, C). The fibrous capsule and the collateral ligaments were partially or completely damaged. Thickened and degenerated capsulo-ligamentous structures could be recognised as inhomogeneous, hypointense ribbon-shaped elements within the tophaceous tissue. MCP tophi expanded dorsally, inducing dislocation of the second finger extensor tendon (Fig. 1), which otherwise showed a normal hypointense signal without discontinuities or lesions. Mild ventral subluxation or complete dislocation of the proximal phalanx of the second finger was another feature. On STIR coronal sequences, bone marrow oedema (BME) was present with involvement of the distal third of the second metacarpal bone and the proximal third of the proximal phalanx of the second finger. Cortical erosions of the second metacarpal head with intraosseous extension of tophaceous tissue were seen.

Tophi of the distal interphalangeal (DIP) joints were observed in two patients. They showed the usual homogeneous low signal intensity pattern on T1-weighted sequences and an almost homogeneous signal intensity pattern on T2-weighted sequences. Capsular collateral ligaments and fibrous capsule could not be appreciated. In addition, an asymmetric, almost circumferential, distribution of tophaceous tissue around the joint was seen, with preserved joint alignment and only minimal reactive BME on STIR sequences (Fig. 2).

In our case series, we analysed two tophi with intratendinous location. One of them induced enlargement of the extensor carpi ulnaris (EUC) tendon and was associated with mild tenosynovitis, dislocation of retinacular structures, and erosions and oedema of

the triquetral base (Fig. 3, 4). On T2-weighted sequences loss of the normal hypointensity of collagen fibres and markedly inhomogeneous intermediate signal intensity were features that heralded tophaceous tissue within the tendon matrix. Otherwise the tendon continuity was preserved, with normal shape and dimensions at the distal insertion site in the fifth metacarpal base. Contrast enhancement was rather homogeneous. In another patient, a small tophus in the proximal patellar tendon induced focal enlargement of the medial aspect of the tendon itself. It was demonstrated as a focus of high signal only appreciable on T2-weighted and STIR sequences.

A heterogeneous signal-intensity pattern was appreciable at T2-weighted sequences of an extra-articular tophus adjacent to the posterior compartment of the elbow (Fig. 5, 6). The spreading of MSU crystals along compartmental and fascial planes was observed here as in most of our examinations. However, in some cases, larger tophi could penetrate through focal discontinuities of superficial fascial layers or deeper compartmental fascial planes. This behaviour may generate at imaging differential diagnosis problems with more aggressive soft tissue neoplastic masses. The contact regions between cortical bone and tophaceous tissue are characterised by a wide spectrum of alterations including periosteal irregularities, cortical thickening, focal cortical discontinuities, and true erosions (Fig. 6). Cortical changes may depend on the antecedent rupture of the fascia. Contrast enhancement was limited only to the solid part of the tophus and not to its fluid portion.

Tophi involving the metatarsophalangeal joint of the great toe, observed in two patients, showed similar signal intensity patterns to the MCP lesions (Fig. 7), but a more heterogeneous signal intensity could be seen both on T1- and T2-weighted sequences when tophaceous tissue contained radiographically confirmed calcified deposits.

Discussion

After years of chronic and untreated hyperuricemia, chronic gouty arthritis can develop with its hallmarks, intrarticular,

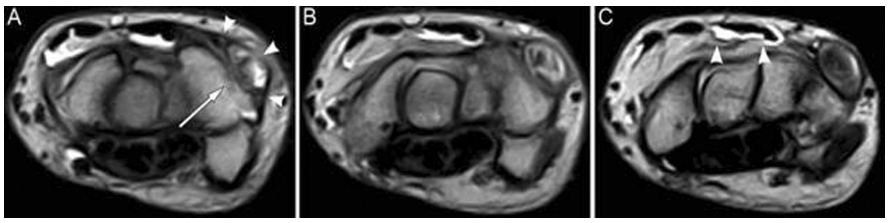

Fig. 3. A, **B**) TSE T2-weighted axial sequences showing marked enlargement of the extensor carpi ulnaris tendon, with a non homogeneous tendon matrix infiltrated by tophaceous tissue. The enlargement of the tendon diameter induces dislocation of the retinacular structures, which are in continuity with the superficial fascial layer (arrowheads). An erosion of the ulnar side of the triquetral bone (arrow), where the enlarged tendon reaches the underlying cortical surface, is shown. **C**) tenosynovitis of the second and fourth extensor tendon compartments (arrowheads).

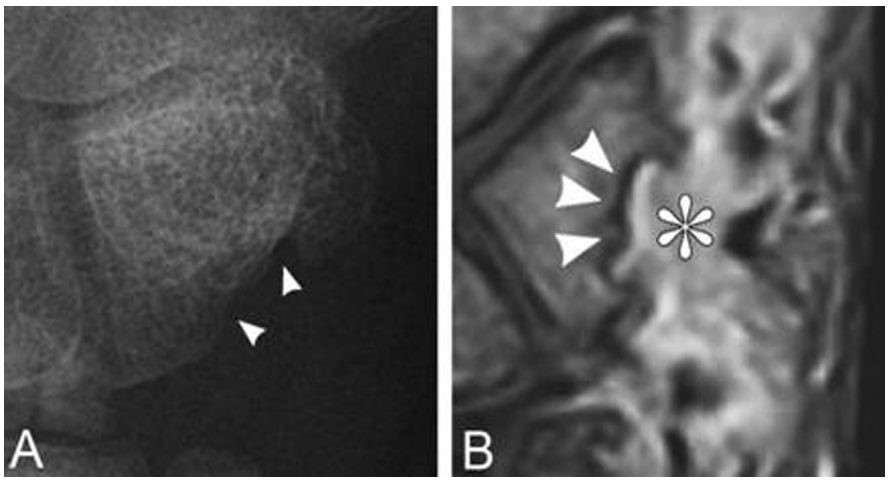

Fig. 4. Same patient as Figure 5: **A**) radiograph demonstrating the erosions on the ulnar side of the base of the triquetral bone (arrowheads). **B**) Gadolinium-enhanced Turbo 3D T1-weighted coronal sequence showing an eterogeneus enhancement of the tophus (asterisk), which is close to the triquetral bone and causes cortical erosions (arrowheads).

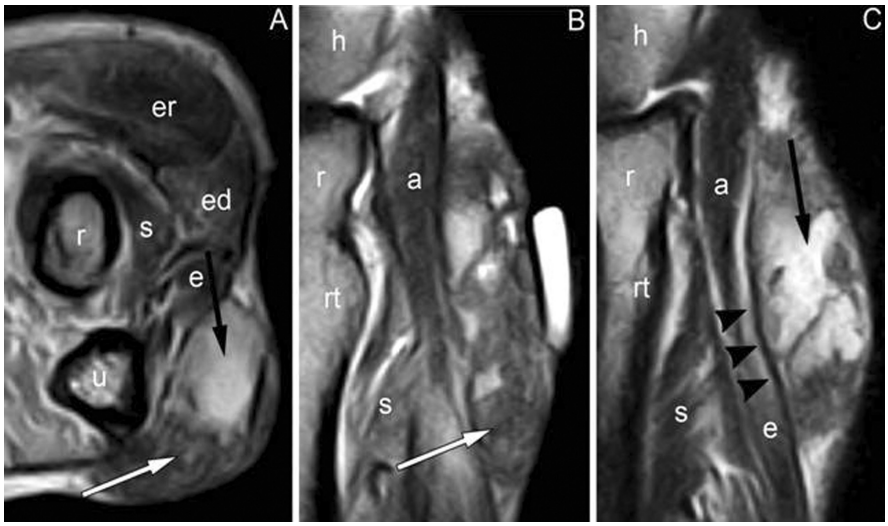

Fig. 5. Large extra-articular tophus adjacent to the posterior compartment of the elbow and to the olecranic bursa. **A**) TSE T2-weighted axial sequence demonstrating two different parts of the tophus: a heterogeneous intermediate to low-signal intensity region (white arrow, see also **B**), on the ulnar side, and a more homogeneous high signal region (black arrow, see also **C**) on the radial side. **B** and **C**) the tophus is in a suprafascial location and compresses the anconeus (a) and extensor carpi ulnaris (e) muscular bellies with its ventral part. The fascial layer is conserved (arrowheads). (s: supinator muscle; h: capitulum humeri; r: radial capitellum; rt: radial tubercle; ed: extensor digitorum longus muscle; er: extensor carpi radialis muscle).

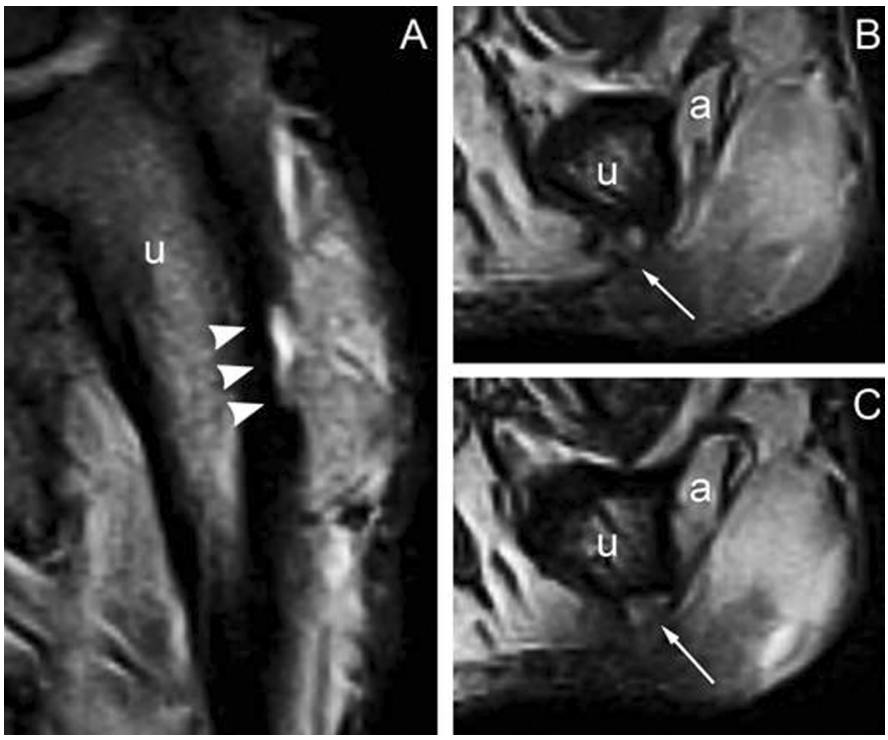

Fig. 6. Same patient as Figure 5 (TSE T2-weighted sequences): **A**) the tophaceous mass shows an almost complete fascial delimitation, but, on its ulnar extremity, a focal interruption of the fascial layer (arrowheads) is seen. **B** and **C**) a subtle expansion of the tophus damaging the posterior cortical surface of the proximal third of the ulnar diaphysis (arrows) can be seen (U = ulna, a = anconeus muscle).

periarticular, intraosseous and soft tissue tophi. At histologic analysis, tophi are foreign body granulomas consisting of MSU deposits surrounded by highly vascularised inflammatory tissue rich in histiocytes, lymphocytes, fibroblasts, and foreign-body giant cells (16, 17). MSU deposits may be intra-articular in hyaline cartilage, subchondral bone, synovial membrane and other synovial spaces, including communicating and non-communicating bursae, or para- or juxta-articular in capsulo-ligamentous structures, ligaments, tendons and subcutaneous tissues (4).

In the literature there are only occasional papers dealing with the MRI appearance of tophi in the peripheral joints (8, 10-14), but none of them employs low-field MRI.

Tophi showed homogeneous low signal intensity, similar to that of muscle, on T1-weighted images, and variable signal intensity on T2-weighted images, although an intermediate to low heterogeneous signal intensity pattern is considered the most common (2). In our experience, the size of the tophus correlated with T2 signal intensity because larger tophi showed a more heterogeneous signal intensity pattern whereas smaller ones had a homogeneous signal. This variable signal intensity pattern could be due to differences in calcium concentration, including bone debris, within the tophus (10, 16). Since calcification of tophi is relatively uncommon (and was not seen in our patients except for one with MTP tophus), this variability could more often result from the presence of MSU and fibrous tissue, including capsuloligamentous debris (18). In particular fibrous tissue, crystals and hemosiderin are supposed to be responsible of low intensity areas within tophaceous tissue on T2-weighted sequences (12). The effects of the ferromagnetic properties of haemosiderin are emphasised with gradient-recalled echo sequences because of the differences in magnetic susceptibility between haemosiderin and adjacent tissues. This phenomenon, which is called "blooming effect" was not observed in our patients.

Hyperintense signal in T2-weighted sequences may reflect the high protein content of the amorphous centre of the tophus, a feature reported in only one paper (13). We observed a very high signal intensity region on T2-weighted sequences in tophi of the posterior elbow compartment, adjacent to olecranic bursa, and of the patellar tendon.

The pattern of contrast enhancement was variable from intense homogeneous to peripheral and heterogeneous (10). Homogeneous enhancement is the most common reported pattern (2), but a peripheral non-homogeneous pattern is also described, which is in agreement with the histological structure of the tophus (10). In the three patients who could perform gadolinium enhancement, we found a heterogeneous pattern in one, an homogeneous pattern in the solid part of the tophus in another one, and a peripheral thin line of marked enhancement, suggesting the presence of highly vascularised tissue, such as granulation or synovial tissue, in the third patient. By contrast, the central portion, which is usually characterised by an amorphous matrix with high protein and MSU crystals content, showed a low or absent enhancement. Although contrast enhancement was obtained only in three patients, these findings indicate a wide variability of the related pattern.

In chronic gout, erosions and BME are usually closely associated with tophi. Erosions are probably result of MSU-induced osteoclast activation (19). The MRI pattern of BME in chronic tophaceous gout has been only rarely described. In our case series, BME adjacent to tophi was seen in 7/9 patients suggesting that it is rather common in this condition. Since BME is reported as a sign of disease activity in RA, it could be related to subclinical inflammation associated with the contact with tophi in gout. BME was absent in the patient with pure intratendinous location of the tophus and in the one with tophus of the elbow. In both fibrous tissue separated the tophus from the adjoining bone.

MRI studies have also shown that urate deposits spread along compartmental and fascial planes, rather than in a radial pattern (14). This point was confirmed in our examinations, although large tophi infiltrated on occasion focal discontinuities of the superficial fascial layers or deeper compartmental fascial

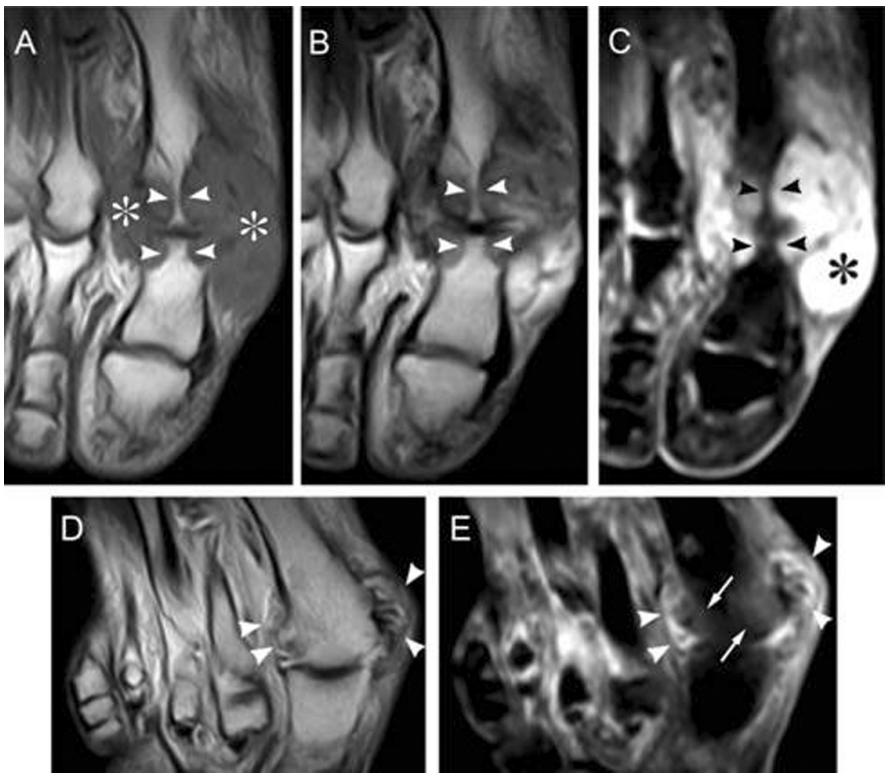

Fig. 7. A) SE T1-weighted coronal sequence of the left forefoot showing homogeneous intermediate signal intensity pattern of an intra-articular tophus of the first metatarsophalangeal joint with extension in the surrounding soft tissues. Deep erosions of the first metatarsal head and of the base of the proximal phalanx are present (arrowheads). **B**) TSE T2-weighted coronal sequence showing a heterogeneous intermediate to low signal intensity pattern. **C**) On the STIR coronal sequence a heterogeneous high signal intensity pattern is observed with a region of fluid-like signal intensity on the medial aspect of the tophus, adjacent to the phalanx base (asterisk). Bone marrow oedema is also present. **D** and **E**) coronal TSE and STIR images of a tophus of the first MTP joint in another patient: note the dishomogeneous appearance of the tophaceous deposit (arrowheads), most probably due to calcification foci that were confirmed on radiographs. Bone marrow edema is also shown (arrows).

planes. Weakening of tendons and ligaments by the presence of tophi, a condition predisposing to tendon rupture, has been reported (1). In our case series, infiltration and damage of tendons, joint capsula, and ligaments by granulomatous tissue was a variable feature. Capsuloligamentous structures were more prone to infiltration and damage than tendons, thus suggesting a robust defensive role of synovial tendon sheath and paratenon against the attack of tophi. Nonetheless, tophi may develop also within the tendons, more often the achilleus or patellar. Intra-tendinous tophi of the hand are rare. The few documented cases have mainly occurred in the extensor tendons of the fingers or in the flexor tendons in the palm or the wrist (11, 20), but not in the EUC tendon, as observed in one of our patients. This study is in keeping with the patterns of tophaceous deposition described by Popp *et al*. (11), *i.e*. discrete nodular, compartmental deposit, or the permeative spread, infiltrating the surrounding structures. Follow-up studies with MRI should be performed to demonstrate if these patterns are determined by the location of the tophus, by disease duration and severity, or by other unknown individual factors.

This is the first study investigating gout with an extremity-dedicated MRI system, except for our previous report on gouty dactylitis (21). Extremity-dedicated MRI is a relatively cheap procedure, which is well accepted even by claustrophobic patients. It is well-suited for the study of tophi who are almost always located in the limbs. The accuracy of low-field, dedicated machines in arthritis, as compared with high-field machines, is debated (22). However, several studies have shown that both are comparable for the evaluation of synovitis and erosions of the hand in RA patients (23, 24). The sensitivity of dedicated MRI for the detection of BME may be lower, although it has progressed with the introduction of new sequences. We cannot exclude that bone edema could be underestimated in our study. In addition, extremity-dedicated MRI, using the same system employed in our study, reliably detects bone erosions when compared with high-resolution CT (25, 26).

Our study has several limitations: the number of patients examined was relatively small, although comparable to that of previous studies with high-field MRI-machines (8, 11, 12). No direct comparison with high field MRI systems has been performed in our study, but the MRI pattern observed is similar to that reported in the literature, therefore suggesting that extremity-dedicated MRI is a good tool to investigate tophi. Turbo-three-dimensional T1-weighted coronal sequence, with isotropic acquisition (0.6 mm minimum voxel size) and multiplanar reconstructions, effective to detect bone changes, short tau inversion recovery sequence, extremely water-sensitive and able to show BME, as well as spin echo sequence able to investigate fibrous tissues, were helpful.

In a recent paper, we have shown that sonoelastography may help discriminating tophi from rheumatoid nodules (27). To gain insight into the potential of MRI in differential diagnosis, we have studied also a typical rheumatoid nodule. As reported in the literature (28), it showed an intermediate to low signal intensity on T1-weighted images with heterogeneous striated and lamellar architecture (Fig. 8), which was not observed in gout tophi. On T2 weighted sequences its appearance was variable, ranging from near homogeneous low signal intensity to heterogeneous high signal intensity. Bone marrow edema and bone cortex erosions were not present adjacent to the rheumatoid nodule. Although a specific MRI feature of rheumatoid nodules was not identified, the lamellar architecture and the absence of BME could represent an important differential aspect.

In conclusion, we have described the MRI appearance of gout tophi using an

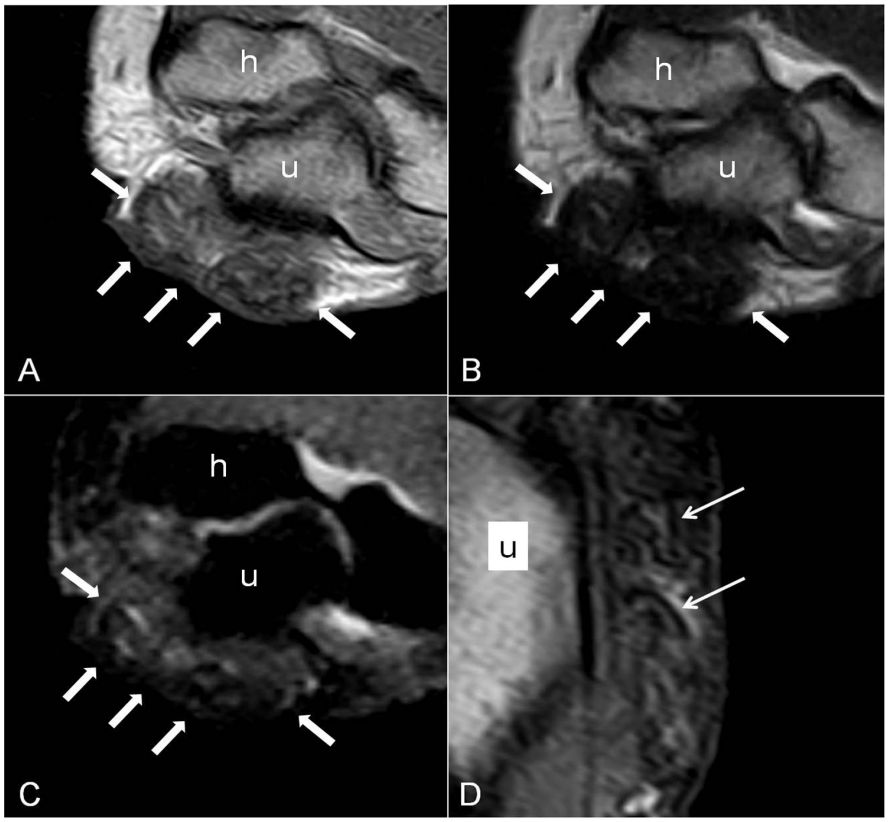

Fig. 8. MRI images of a subcutaneous rheumatoid nodule (large arrows) of the posterior elbow compartment. On the SE T1-weighted image (**A**), an intermediate to low signal intensity is seen with a heterogeneous striated or lamellar internal architecture. On the FSE T2-weighted (**B**) and STIR (**C**) sequences, the nodule shows low signal intensity. The SE T1-weighted sagittal sequence (**D**) demonstrates the low signal intensity septa within the nodule (small arrows) (u = ulna, h = humerus).

extremity-dedicated machine. We do not claim that MRI should be systematically employed for the diagnosis of gout. Nonetheless, it could be useful in selected cases to demonstrate clinically invisible tophi. This technique may also help in the differential diagnosis of nodules and in the patients' follow-up by measuring the size of the tophi during hypouricaemic treatment (12). MRI is also important to investigate the pathogenesis of gout and to better understand its clinical progression.

References

1. MONU JUV, POPE TL, JR. Gout: a clinical and radiologic review. *Radiol Clin N Am* 2004; 42: 169-84.
2. ROSENBERG AE: Crystal arthropathies. *In*: COLTRAN RS, KUMAR V, ROBBINS SL, SCHOEN FJ, editors. *Robbins' pathologic basis of disease*. 5th edition. Philadelphia: W.B. Saunders; 1994. p. 1255-8.
3. DALBETH N, MCQUEEN FM: Use of imaging to evaluate gout and other crystal deposition disorders. *Curr Opin Rheumatol* 2009; 21: 124-31.
4. GENTILI A: The advanced imaging of gouty tophi. *Curr Rheumatol Rep* 2006; 8: 231-5.
5. WORTMANN RL: Gout and hyperuricemia. *In*: FIRESTEIN G, ed. *Kelley's Textbook of Rheumatology*. Philadelphia: Saunders Elsevier, 2008: 1481-524.
6. CHOI M H, MACKENZIE J, DALINKA M K: Imaging features of crystal-induced arthropathy. *Rheum Dis Clin N Am* 2006; 32: 427-46.
7. NALBANT S, COROMINAS H, HSU B, CHEN LX, SCHUMACHER HR, KITUMNAYPONG T: Ultrasonography for assessment of subcutaneous nodules. *J Rheumatol* 2003; 30: 1191-5.
8. GERSTER JC, LANDRY M, DUFRESNE L, MEUWLY JY: Imaging of tophaceous gout: computed tomography provides specific images compared with magnetic resonance imaging and ultrasonography. *Ann Rheum Dis* 2002; 61: 52-4.
9. DALBETH N, CLARK B, GREGORY K *et al*.: Mechanisms of bone erosion in gout: a quantitative analysis using plain radiography and computed tomography. *Ann Rheum Dis* 2009; 68: 1290-5.
10. YU JS, CHUNG C, RECHT M, DAILIANA T, JURDI R: MR imaging of tophaceous gout. *AJR Am J Roentgenol* 1997; 168: 523-7.
11. POPP JD, BIDGOOD WD JR, EDWARDS LN: Magnetic resonance imaging of tophaceous gout in the hands and wrists. *Semin Arthritis Rheum* 1996, 25: 282-9.
12. SCHUMACHER HR JR, BECKER MA, EDWARDS NL *et al*.: Magnetic resonance imaging in the quantitative assessment of gouty tophi. *Int J Clin Pract* 2006, 60: 408-14.
13. CHEN CK, CHUNG CB, YEH L *et al*.: Carpal tunnel syndrome caused by tophaceous gout: CT and MR imaging features in 20 patients. *Am J Roentgenol* 2000; 175: 655-9.
14. CHEN CK, YEH LR, PAN HB *et al*.: Intra-articular gouty tophi of the knee: CT and MR imaging in 12 patients. *Skeletal Radiol* 1999; 28: 75-80.
15. WALLACE SL, ROBINSON H, MASI AT, DECKER JL, MCCARTY DJ, YŰ TF: Preliminary criteria for the classification of the acute arthritis of primary gout. *Arthritis Rheum* 1977; 20: 895-900.
16. LIOTÈ F, HANG KORNG EA: Gout: update on some pathogenic and clinical aspects. *Rheum Dis Clin N Am* 2006; 32: 295-311.
17. LLAUGER F, PALMER F, ROSÒN N, BAGUÈ S, CAMINS A, CREMADES R: Nonseptic monoarthritis: imaging features with clinical and histopathologic correlation. *RadioGraphics* 2000; 20: S263-S278.
18. PEREZ-RUIZ F, DALBETH N, ARRESOLA A, DE MIGUEL E, SCHLESINGER N: Imaging of gout: findings and utility. *Arthritis Res Ther* 2009, 11: 232.
19. DALBETH N, SMITH T, NICOLSON B *et al*.: Enhanced osteoclastogenesis in patients with tophaceous gout. Urate crystals promote osteoclast development through interactions with stromal cells. *Arthritis Rheum* 2008; 58: 1854-65.
20. SAINSBURY DCG, HIDVEGI N, BLAIR JW: Intra-tendineous gout in a repaired flexor digitorum profundus. *J Hand Surg* (Eur Vol) 2008; 33: 528-9.
21. ANDRACCO R, ZAMPOGNA G, PARODI M, PAPARO F, CIMMINO MA: Dactylitis in gout. *Ann Rheum Dis* 2010; 69: 316.
22. AMERICAN COLLEGE OF RHEUMATOLOGY EXTREMITY MAGNETIC IMAGING TASK FORCE: Extremity magnetic resonance imaging in rheumatoid arthritis. *Arthritis Rheum* 2006; 54: 1034-47.
23. LINDEGAARD HM, VALLØJ, HØRSLEV-PETERSEN K *et al*.: Low-cost, low-field dedicated extremity magnetic resonance imaging in early rheumatoid arthritis: a 1-year follow-up study. *Ann Rheum Dis* 2006; 65: 1208-12.
24. SCHIRMER C, SCHEEL AK, ALTHOFF CE *et al*.: Diagnostic quality and scoring of synovitis, tenosynovitis and erosions in low-field MRI of patients with rheumatoid arthritis: a comparison with conventional MRI. *Ann Rheum Dis* 2007; 66: 522-9.
25. DUER-JENSEN A, EJBJERG B, ALBRECHT-BESTE E *et al*.: Does low-field dedicated extremity MRI (E-MRI) reliably detect bone erosions in rheumatoid arthritis? A comparison of two different E-MRI units and conventional radiography with high resolution CT scanning. *Ann Rheum Dis* 2009; 68: 1296-302.
26. MØLLER DØHN U, EJBJERG BO J, HASSELQUIST M *et al*.: Detection of bone erosions in rheumatoid arthritis wrist joints with magnetic resonance imaging, computed tomography and radiography. *Arthritis Res Ther* 2008; 10: R25.
27. SCONFIENZA LM, SILVESTRI E, BARTOLINI B, GARLASCHI G, CIMMINO MA: Sonoelastography may help in the differential diagnosis between rheumatoid nodules and tophi. *Clin Exp Rheumatol* 2010; 28: 144-5.
28. STAROK M, EILENBERG SS, RESNICK D: Rheumatoid nodules: MRI characteristics. *Clin Imaging* 1998; 22: 216-9.